

Development of a nano alumina-zirconia composite catalyst as an active thin film in biodiesel production

J Kolae Heydarzadeh¹, N Marzban^{*2}, G D Najafpour³,
M Pourmohammadbagher² & S Valizadeh¹

¹Department of Chemical Engineering,
Islamic Azad University, Shahrood Branch, Shahrood, Iran

²Department of Chemical Engineering,
Isfahan University of Technology, Esfahan, Iran

³Faculty of Chemical Engineering,
Babol Noshirvani University of Technology, Babol, Iran

E-mail: n.marzban@ce.iut.ac.ir

Received 8 May 2016; accepted 12 October 2018

A nano-alumina-zirconia composite catalyst has been synthesized by a simple aqueous sol-gel method using $\text{AlCl}_3 \cdot 6\text{H}_2\text{O}$ and ZrCl_4 as precursors. Thermal decomposition of the precursor and subsequent formation of $\gamma\text{-Al}_2\text{O}_3$ and t-ZrO_2 have been investigated by thermal analysis. XRD analysis show that $\gamma\text{-Al}_2\text{O}_3$ and t-ZrO_2 phases are formed at 700 °C. FT-IR analysis also indicate the phase transition to $\gamma\text{-Al}_2\text{O}_3$ occur in corroboration with X-ray studies. TEM analysis of the calcined powder reveal that spherical particles were in the range of 8-12 nm. The nano alumina-zirconia composite particles are mesoporous and uniformly distributed in their crystalline phase. In order to measure the catalytic activity, esterification reaction has been carried out. Biodiesel, as a renewable fuel, is formed in a continuous packed column reactor. Free fatty acid (FFA) is esterified with ethanol in a heterogeneous catalytic reactor. It is found that the synthesized $\gamma\text{-Al}_2\text{O}_3/\text{ZrO}_2$ composite has the potential to be used as a heterogeneous base catalyst for biodiesel production processes.

Keywords: Nano alumina-zirconia, Composite catalyst, Thin film, Biodiesel

Nowadays, several catalytic reactions such as base catalyzed esterification¹⁻³, acid-catalyzed esterification^{4,5}, enzymatic esterification^{6,7} and heterogeneous catalyst esterification^{8,9} are used for biodiesel production from free fatty acids (FFAs). Now, the homogeneous catalysts are being extensively used for the production of biodiesel at industrial, scale such as sulfuric acid, the most common homogeneous catalyst consumed in biodiesel synthesis¹⁰. The use of the homogeneous catalysts, however, has some disadvantages. One of the most obvious disadvantages of homogenous catalysts is that they should be eliminated from the final product by repeated washing with distilled water, thereby

causing the formation of a massive amount of wastewater. In order to overcome such problems, heterogeneous catalysts are applied. Heterogeneous catalysts can be easily separated from the final product and used several times. Alumina is widely used as a catalyst due to its favorable catalytic properties¹¹. In particular, γ -alumina, which has large surface area and suitable pore size distribution, is an important catalyst for binding organic compounds¹². Zirconia is one of the additives which can increase the strength and toughness of the alumina matrix either by stress-induced transformation toughening or microcrack toughening¹³. Zirconia was selected due to its chemical inertness (compared to other oxide phases), intrinsic catalytic activity (higher than other classical supports like pure Al_2O_3 or SiO_2) and the thermal stability of the $\text{Al}_2\text{O}_3\text{-ZrO}_3$ composite system^{14,15}. On the other hand, it was also shown that alumina delayed the crystallization, increased the specific surface area and pore volume, and enhanced the surface acidity of zirconia¹⁶. Several methods for the preparation of the alumina-zirconia nanopowders and composites have been reported in the literature¹⁷⁻²¹. The sol-gel process is one of the most useful techniques used to offer the possibility of making ultra homogeneous structures and it has been widely used in the synthesis of glasses, ceramics and composites catalysts^{15,17}. Sol-gel method is also used for preparing the gels of various shapes such as monoliths, fibers, coating films, spheres, etc. It is well known that the composition of the starting alkoxide solution, including the type of catalyst, water content, the presence or absence of any additives and the reaction conditions, directly affects the rate of hydrolysis, the rate of condensation, the shape of produced polymer particles in the solution and the state of aggregation of particles, respectively. Thus, characteristics of the sols and gels produced in the reaction could be easily changed by varying several parameters. Sol-gel method, among different coating methods used, has shown promising results due to its low cost, simple control of the synthesized parameters and the ability to form a uniform coating over large or complex geometric shapes physically and chemically. It has the potential to enhance physical and chemical properties due to the nanocrystalline structure of the

coatings^{16,17}. Several investigators have used solutions/sols of alumina and zirconia salts or suspensions of Al₂O₃ and ZrO₂ powders to control the particle size of ZrO₂ and Al₂O₃²⁰. In this research, the sol-gel method was used to synthesize a nano thin film of alumina-zirconia composite catalysts. Prepared samples obtained through sol-gel technique were then characterized by BET surface area, TEM, XRD, FTIR and AFM analysis. The purpose of the present research was to develop an effective catalytic process for biodiesel production using nano alumina-zirconia composite as an active thin film.

Experimental Section

Preparation of Al₂O₃/ZrO₂ composite catalyst thin film

In order to synthesize Al₂O₃/ZrO₂ nanocomposite particles, aluminum chloride hexahydrate (AlCl₃.6H₂O), zirconium (IV) chloride (ZrCl₄), yttrium (III) nitrate (Y(NO₃)₃.6H₂O), citric acid (C₆H₈O₇) and ethylene glycol (HOCH₂CH₂OH) were prepared by the sol-gel method. All materials were supplied by Merck (Darmstadt, Germany). Figure 1 shows the stepwise procedures employed for the preparation of the nanocomposite particles and the thin film by the sol-gel method. The mixture of the solutions was relatively stable, i.e., no precipitation or phase separation was observed during the process.

Ceramic plates were used as the substrate material. The substrates were coated by dip-coating technique and withdrawn in the solutions at a constant speed of about 1 mm/s. The coated substrates were allowed to be dried at 70°C for 12 h. The coated plates were then calcinated at 700°C with a heating rate of 5°C/min to the distinctive temperature and maintained for 5 h.

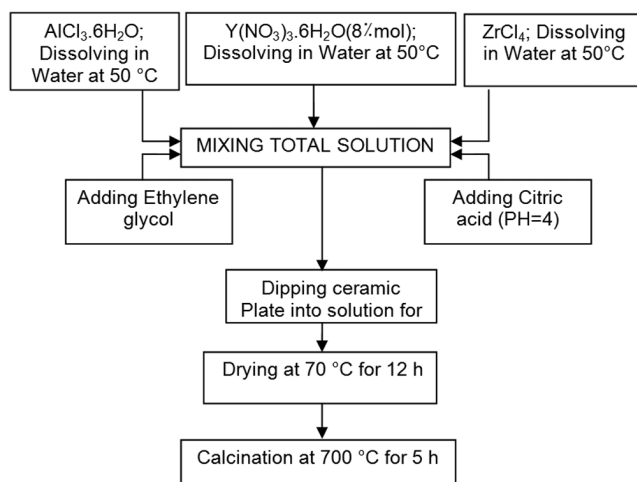


Fig. 1 — Typical flow chart of processing nanocomposite Al₂O₃-ZrO₂ thin film.

Catalyst characterizations

The morphology of the calcinated powders of the thin film were investigated using a Philips EM208S transmission electron microscope (TEM). For the phase analysis of the thin film, X-ray diffraction (XRD, Siemens D500 Model) with Cu-K α radiation in the range of 10–70 and at scanning steps of 2 θ =4 °/min was used. The crystalline size of the synthesized particle was calculated using Scherrer's equation as stated below²¹:

$$D = \frac{0.9 \lambda}{B \cos \theta}$$

where D is the crystalline size (nm), λ is the wavelength of X-ray radiation (1.54056 Å), θ is the Berg's angle, and B is the full width at half maximum. The BET surface area of the thin film in air was determined at 700°C for 5 h by a surface analyzer model (Gemini 2375, USA) using N₂ as the adsorbate. Fourier transform infrared spectroscopy (FTIR) analysis of the thin film was carried out in a Nicolet Nexus 6700 spectrometer and in the wave number range of 400-4000 cm⁻¹ to study the chemical groups. The surface morphology of the thin film was examined by an Auto Probe model CP atomic force microscope (AFM, Park scientific instruments, USA) using a Si₃N₄ probe.

Reaction test

The esterification process was carried out in a continuous packed bed reactor. The column was packed and loaded with palletized catalysts (600 g, γ -Al₂O₃/ZrO₂). About 82% of the reactor volume was occupied by the palletized catalysts. Fatty acids mixture and ethanol were primarily heated up to 50°C in a mixing tank. The fatty acids were pumped to the top of the column. The FFA met and interacted with ethanol on the active sites of catalysts and the ester product was instantaneously formed. The product was transferred to a flash drum separator²².

Result and Discussion

A transmission electron microscope (TEM) was used to analyze the particle size and morphology of the nanocomposite powder particles. Figure 2 shows the micrograph of alumina-zirconia composite powders synthesized using sol gel method and calcined at 700°C for 5 h. Most particles were in the range of 10-15 nm. The phenomenon of meso-porosity within particles could also be observed in this TEM picture and most particles were spherical in nature. TEM studies showed

powder agglomeration. Generally, it can be said that the increase in Specific Surface area may improve the catalytic activity. The specific surface area of the final composite powders was determined by the BET surface area analysis and the calculated surface area was about $\sim 120 \text{ m}^2/\text{g}$. The X-Ray diffraction pattern has been shown in Fig. 3. It indicated that the calcined coating seemed to be amorphous. This might be due to the organic compounds of the coating. The strong peak at $2\theta=30.2^\circ$ was assigned to the (111) lattice plan whereas the other weak peak at $2\theta=35.11^\circ$, 50.65° , 60.17° , and 63.10° could be ascribed to (200), (220), (131), and (222) lattice planes of tetragonal Zirconia

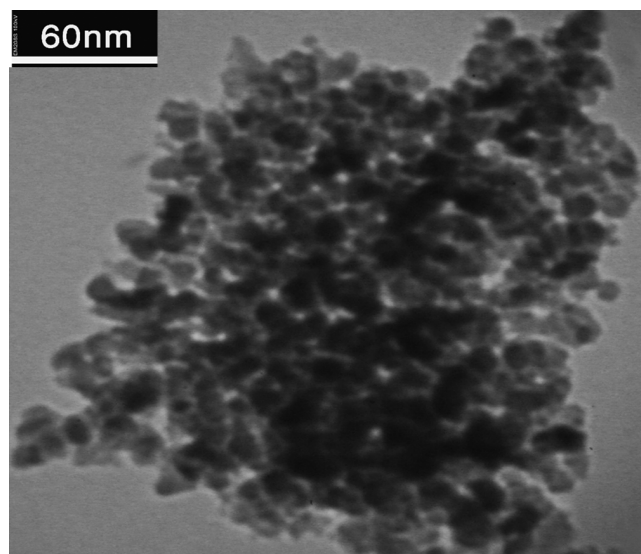


Fig. 2 — Transmission electron micrographs of the alumina-zirconia particles after calcination at 700°C for 5 h.

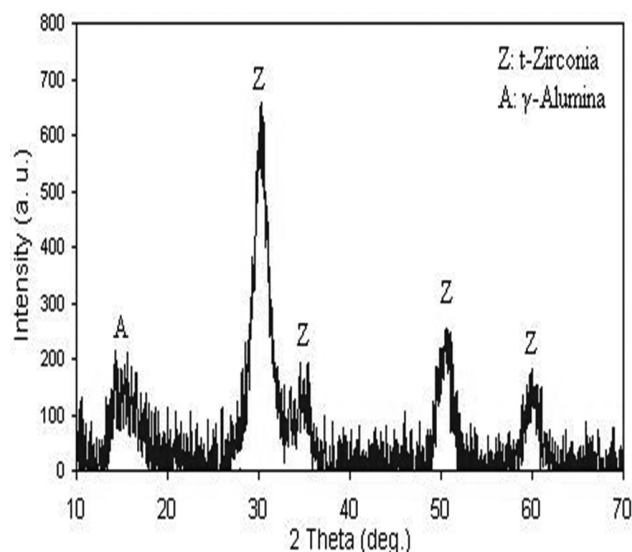


Fig. 3 — Phase analysis of the synthesized coating after calcination at 700°C .

(t- ZrO_2) phase, respectively. The stabilization of t- ZrO_2 could be attributed to the structural similarity of the dopant, Y_2O_3 , ZrO_2 and the larger dopant cation radius compared with the Zr^{4+} radius²³. The yttria was changed into yttrium oxide when exposed to the high temperature (700°C). Another explanation for the stabilization of the tetragonal phase of zirconia in Y_2O_3 doped ZrO_2 system could be based on the formation of oxygen vacancies resulting from the presence of trivalent cation^{24,25}. Also, the strong peak at $2\theta=14.7^\circ$ was assigned to the lattice plan whereas the other weak peak at $2\theta=54.2^\circ$, and 55.3° could be ascribed to the lattice planes of $\gamma\text{-Al}_2\text{O}_3$. It can be concluded that the prepared nanopowders have obviously different crystal structures. The alumina was diffused into the zirconia lattice, stabilizing the crystal phase of zirconia in the sample. The broadening of peaks in XRD pattern confirmed that the average crystallite size was small. The crystallite size of the calcined powder was calculated using Scherrer's equation and the size varied between 5 nm and 15 nm.

Fourier transform infrared spectroscopy (FTIR) analysis for the synthesized composite in the wave number region of $4000\text{-}400 \text{ cm}^{-1}$ is shown in Fig. 4. The band located at $\sim 3440 \text{ cm}^{-1}$ was attributed to the O–H stretching vibration and the band at $\sim 1640 \text{ cm}^{-1}$ was related to the H–O–H symmetric stretching vibration of adsorbed water molecules. The absorption bands centered at ~ 600 and $\sim 800 \text{ cm}^{-1}$ were assigned to the Al–O bonding vibration in tetrahedral and octahedral environments respectively, suggesting $\gamma\text{-alumina}$ ²⁶. Also, the band at 480 cm^{-1} corresponded to the vibration absorption of Zr–O bond in tetragonal

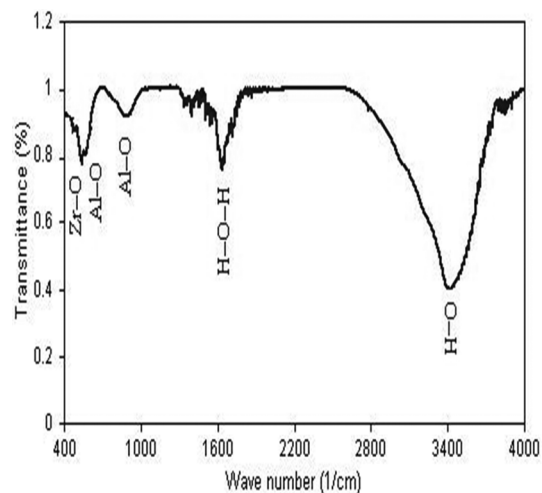


Fig. 4 — FTIR curves of $\text{Al}_2\text{O}_3/\text{ZrO}_2$ coating after calcination at 700°C .

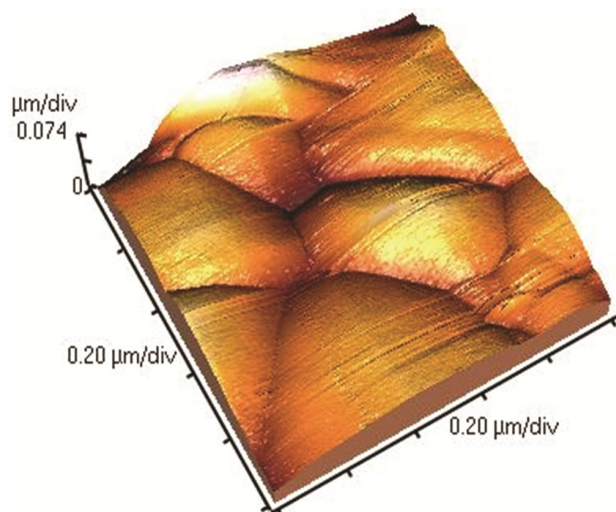


Fig. 5 — AFM images of coating $\text{Al}_2\text{O}_3/\text{ZrO}_2$ composite on the ceramic plate.

zirconia. This can be explained by the relative contribution of two bonds, Zr–O and Al–O bonds, and it is consistent with the formation of $\text{ZrO}_2\text{–Al}_2\text{O}_3$. This supports the XRD results and the formation of Alumina and zirconia in the present study.

Atomic Force Microscope (AFM) images of the thin coating $\text{Al}_2\text{O}_3/\text{ZrO}_2$ composite on the ceramic plate are shown in Fig. 5. It demonstrated that the surface of the alumina-zirconia coating was compact. The coating was crack-free and consisted of nano scale crystallites. However, the surface of the coated $\text{Al}_2\text{O}_3/\text{ZrO}_2$ composite was uneven and sinusoidal, but the roughness of the catalyst was less than 10 nm.

Esterification reactions

The rate of esterification was strongly influenced by the mass ratio of fatty acid to ethanol. Since the esterification process was reversible, the yield of ethyl esters produced was favored with the excess amount of ethanol. In order to obtain an optimal mass ratio for this process, five experiments were carried out with variable free fatty acid/ethanol mass ratios, between 1:5 and 3:5. Figure 6 shows the conversion of FFA to ethyl ester as a function of the mass ratio of FFA/ETOH. However, the presented data demonstrated that at a mass ratio of 3:5, the maximum ester yield was obtained. Increasing the mass ratio from 1:1 to 3:5 raised the conversion of ester formation from 25 to 90%. Also, ethyl ester formation was strongly dependent on the reaction temperature. To evaluate the effect of reaction temperature on the production of ethyl esters, the esterification process was carried out under optimal conditions. Esterification could be conducted at various temperatures. In most cases, the

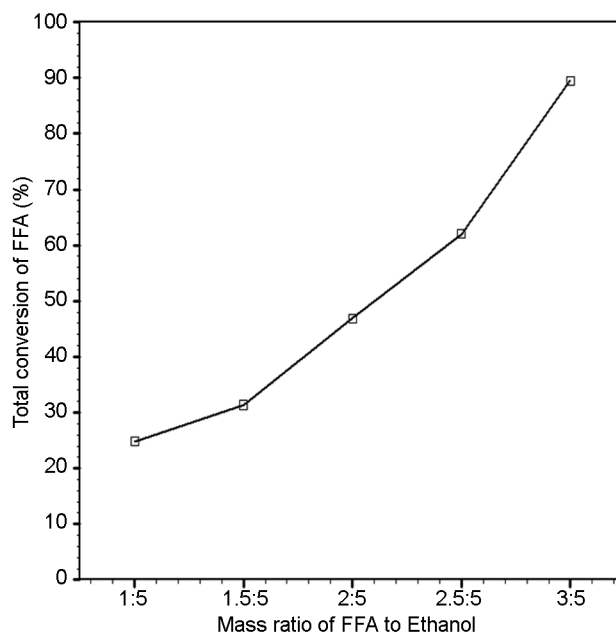


Fig. 6 — Conversion of FFA to ethyl ester as a function of the mass ratio of FFA/ETOH.

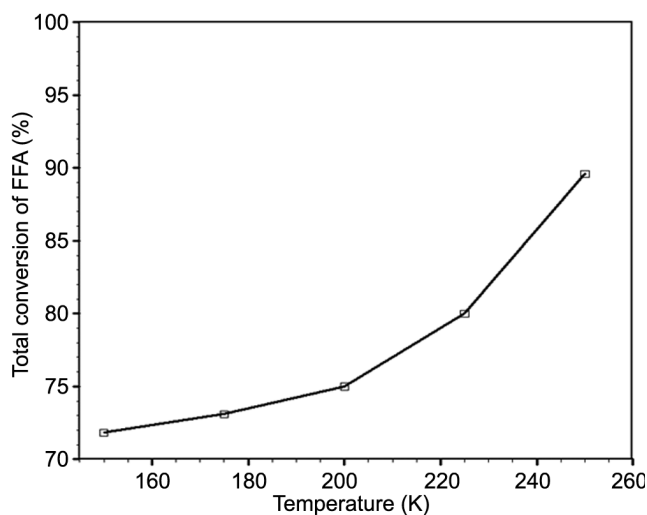


Fig. 7 — The effect of temperature on the yield of ethyl ester.

temperature has been kept close to the boiling point of alcohol used in the process²⁷. However, high temperatures can reduce the reaction time. In this research, temperature was varied in the range of 150–250°C. As shown in Figure 7; the results indicated that increasing the reaction temperature had a favorable influence on the yield of ethyl ester formation.

Conclusion

In this study, A new heterogeneous base composite catalyst has been examined in order to develop an effective catalyst for biodiesel production. A novel

sol-gel technique has been developed in which the alumina and zirconia sol could be prepared at room temperature from the inorganic salts. This process can be used to prepare uniform mesoporous alumina-zirconia composites. The present work demonstrate the manufacture of a nano film γ -Al₂O₃-ZrO₂ composite coated on ceramics plates through the sol-gel route. The heterogeneous catalytic reactor has a great ability to produce biodiesel fuel within a short reaction time. It can be concluded that as the mass ratio of FFA/ethanol is increased, the reaction yield and conversion of free fatty acid are also increased. The maximum reaction yield at the mass ratio of 3:5 was 90%. At the high temperature (250°C), high reaction conversion is reached. As expected, at the low temperature, the conversion is low. With the implementation of optimal operational condition, the maximum yield of approximately 90% is achieved. These results show the possibility for this composite catalyst to act as an effective heterogeneous base catalyst for the manufacture of biodiesel.

References

- 1 Leung D Y C, Wu X & Leung M K H, *Appl Energ*, 87 (2010) 1083.
- 2 Liu X, He H, Wang Y, Zhu S & Piao X, *Fuel*, 87 (2008) 216.
- 3 Lam M K, Lee K T & Mohamed A R, *Biotechnol Adv*, 28 (2010) 500.
- 4 Miao X, Li R & Yao H, *Energ Convers Manage*, 50 (2009) 268.
- 5 Jain S & Sharma M, *Bioresour Technol*, 101 (2010) 7701.
- 6 Ognjanovic N, Bezbradica D & Knezevic-Jugovic Z, *Bioresour Technol*, 100 (2009) 5146.
- 7 Shah S & Gupta M N, *Process Biochem*, 42 (2007) 409.
- 8 Kim H J, Kang B S, Kim M J, Park Y M, Kim D K, Lee J S & Lee K Y, *Catal Today*, 93 (2004) 315.
- 9 Xie W & Li H, *J Mol Catal A Chem*, 255 (2006) 1.
- 10 Lopez D E & Goodwin J G, *Appl Catal A Gen*, 295 (2005) 97.
- 11 Marandi V & Najafpour G D, *Int J Eng Sci Technol*, 12 (2001) 1.
- 12 Liu Q, Wang A, Wang X, Gao P, Wang X & Zhang T, *Microporous Mesoporous Mater*, 111 (2008) 323.
- 13 Sarkar D, Mohapatra D, Ray S, Bhattacharyya S, Adak S & Mitra N, *Ceram Int*, 33 (2007) 1275.
- 14 Dominguez J, Hernandez J & Sandoval G, *Appl Catal A Gen*, 197 (2000) 119.
- 15 Enache D, Roy-Auberger M, Esterle K & Revel R, *Colloids Surf A Physicochem Eng Aspects*, 220 (2003) 223.
- 16 Feth M P, Bauer M, Kickelbick G, Metelkina O, Schubert U & Bertagnolli H, *J Non Cryst Solids*, 351 (2005) 432.
- 17 Khalil N, Hassan M, Ewais E & Saleh F, *J Alloys Compd*, 496 (2010) 600.
- 18 Jayaseelan D D, Rani D A, Nishikawa T, Awaji H & Gnanam F, *J Eur Ceram Soc*, 20 (2000) 267.
- 19 Bartolomé J F, Pecharrromón C, Moya J S, Martegn A, Pastor J Y & Llorca J, *J Eur Ceram Soc*, 26 (2006) 2619.
- 20 Weng M T, Wei W C J & Huang C Y, *Key Eng Mater*, 353 (2007) 540.
- 21 Klug H P & Alexander L E, *X-Ray Diffraction Procedures: For Polycrystalline and Amorphous Materials*, 2nd Edition, (Wiley-VCH), 992 (1974).
- 22 Heydarzadeh J K, Amini G, Khalizadeh M A, Pazouki M, Ghoreyshi A A, Rabiee S M & Najafpour G D, *World Appl Sci J*, 9 (2010) 1306.
- 23 Del Monte F, Larsen W & Mackenzie J D, *J Am Ceram Soc*, 83 (2000) 1506.
- 24 Das D, Mishra H, Parida K & Dalai A, *J Mol Catal A Chem*, 189 (2002) 271.
- 25 Raz S, Sasaki K, Maier J & Riess I, *Solid State Ionics*, 143 (2001) 181.
- 26 Macedo M I F, Osawa C C & Bertran C A, *J Sol Gel Sci Technol*, 30 (2004) 135.
- 27 Fernando S, Karra P, Hernandez R & Jha S K, *Energy*, 32 (2007) 844.